# Dramatically Enhanced Oxygen Fluxes in Fluorite-Rich Dual-Phase Membrane by Surface Modification

**ARTICLE** *in* CHEMISTRY OF MATERIALS · AUGUST 2014

Impact Factor: 8.35 · DOI: 10.1021/cm501240f



**6 AUTHORS**, INCLUDING:

Jong Hoon Joo
Chungbuk National University
**44** PUBLICATIONS **449** CITATIONS
SEE PROFILE

Younki Lee
Research Institute of Industrial Science and Te…
**11** PUBLICATIONS **42** CITATIONS
SEE PROFILE

Chung-Yul Yoo
Korea Institute of Energy Research
**35** PUBLICATIONS **164** CITATIONS
SEE PROFILE

Ji Haeng Yu
Korea Institute of Energy Research
**63** PUBLICATIONS **783** CITATIONS
SEE PROFILE

CHEMISTRY OF MATERIALS

Article

pubs.acs.org/cm

# Dramatically Enhanced Oxygen Fluxes in Fluorite-Rich Dual-Phase Membrane by Surface Modification

Jong Hoon Joo,*[,†] Kyong Sik Yun,[‡] Younki Lee,[†,§] Jaewon Jung,[†] Chung-Yul Yoo,[†] and Ji Haeng Yu*[,†]

[†]Advanced Materials & Devices Laboratory, Korea Institute of Energy Research, 152 Gajeong-ro, Daejeon 305-343, Republic of Korea

[‡]Department of Material Science and Engineering, Chungnam National University, Daejeon 305-764, Republic of Korea

**ABSTRACT:** Dual-phase ceramic membranes with very high oxygen flux have been designed by taking into account the volume fraction of the fluorite phase, membrane thickness, and surface modification. The oxygen flux of $Ce_{0.9}Gd_{0.1}O_{2-\delta}$–$La_{0.6}Sr_{0.4}Co_{0.2}Fe_{0.8}O_{3-\delta}$ (GDC–LSCF) dual-phase membranes has been systematically investigated as a function of membrane thickness and volume fraction of the fluorite phase with or without surface modification. The percolation threshold of the composites for electronic conduction has been determined to be about 20 vol % of LSCF by general effective-medium theory. The oxygen flux of uncoated fluorite phase-rich membrane (80 vol % GDC–20 vol % LSCF) with 30-$\mu$m thickness exhibits a low oxygen flux ($8.0 \times 10^{-3}$ mL·cm$^{-2}$·min$^{-1}$ at 850 °C) under an air/He gradient, indicating that the permeation is controlled by only the surface-exchange kinetics of GDC. With both sides coated with $La_{0.6}Sr_{0.4}CoO_{3-\delta}$ (LSC), the flux of the membrane (3.6 mL·cm$^{-2}$·min$^{-1}$ at 850 °C) has been dramatically enhanced by about 3 orders of magnitude in comparison with the oxygen flux of the membrane with a nonmodified surface. This observation implies that surface modification has a decisive role in dramatically enhancing the contribution of the GDC to the fluorite rich dual-phase membrane.

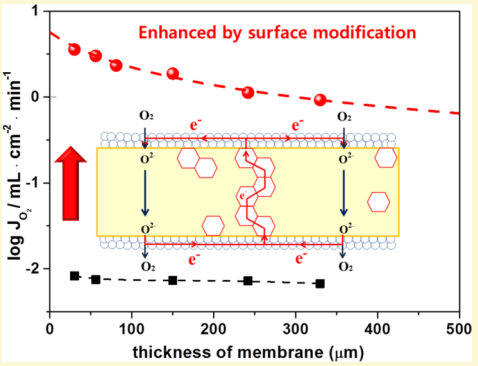


## 1. INTRODUCTION

In recent years, the demand to reduce $CO_2$ emissions has spurred the rapid development of $CO_2$ capture and storage technologies. Since coal-fired power plants are one of the biggest sources of $CO_2$ emissions, the technology for coal-fired power generation with $CO_2$ capture has become an increasingly important area of research.[1−3] The promising concepts for coal-fired power generation with $CO_2$ capture are usually divided into three categories: postcombustion capture, precombustion separation, and oxy-fuel combustion capture.[4,5] Ceramic oxygen ion conducting membranes with high oxygen permeability have recently received increased attention since they can be a promising candidate to supply pure oxygen to oxy-fuel plants for $CO_2$ capture.[6−8] In particular, perovskite materials such as $Ba_{0.5}Sr_{0.5}Co_{0.8}Fe_{0.2}O_{3-\delta}$ (BSCF) have been intensively investigated because of their high oxygen permeability.[9−11] However, their thermochemical and mechanical instability limits their application in oxygen permeation membrane. Their high thermal expansion coefficient (TEC), which is normally above $20 \times 10^{-6}$ K$^{-1}$, can also lead to cracking and delamination of the membranes.[12,13] To overcome the problems of single-phase perovskite, there have been intensive studies on dual-phase composite membranes that consist of a fluorite phase as an oxygen-ion conductor and a perovskite material as an electronic and ionic conductor.[14−18] Because fluorite materials used as electrolytes in solid-oxide fuel cells (SOFCs) have thermochemical stability under reducing and $CO_2$ atmospheres, fluorite-based composites can enhance the chemical stability of ceramic membranes for oxygen separation. In addition, since the TEC values of fluorite oxides (about 10–$12\times 10^{-6}$ K$^{-1}$) are relatively low compared to those of perovskite oxides, fluorite-based composites can enhance the mechanical stabilities of the membrane. Fluorite oxide also shows negligible a chemical expansion at an oxygen partial pressure gradient (air/He or air/vacuum); fluorite-rich dual-phase membrane has a beneficial effect on the mechanical stability when the membrane is exposed to a gradient of oxygen chemical potential. A minimum amount of the perovskite phase in dual-phase membranes is also required, while maintaining adequate electronic conduction, in order to improve the overall stability of the membrane. Even though a number of reports on dual-phase membranes have been published, the contribution of the fluorite phase to oxygen permeability from the viewpoint of surface-exchange kinetics is still poorly understood. In addition, most studies in dual-phase membrane have only been carried out in the millimeter-thickness range, which can lead to little understanding of the effect of surface-exchange kinetics on oxygen permeation.[19−21] In our study, in order to comprehend the contributions of the fluorite phase, the oxygen flux of thin-film-based dual-phase membranes (Gd-doped ceria (GDC), $Ce_{0.9}Gd_{0.1}O_{2-\delta}$–$La_{0.6}Sr_{0.4}Co_{0.2}Fe_{0.8}O_{3-\delta}$ (GDC–LSCF), was investigated with decreasing membrane thickness to 30 $\mu$m with or without surface modification. The GDC as an oxygen-ion conductor and the LSCF as an electronic and ionic

Received: April 8, 2014
Revised: July 2, 2014
Published: July 3, 2014

   dx.doi.org/10.1021/cm501240f | Chem. Mater. 2014, 26, 4387−4394

conductor are chosen because these materials are state-of-the art for SOFC materials. To the best of our knowledge, this is the first report on the oxygen flux of free-standing thin-film membranes (minimum thickness ~30 $\mu$m). The effects of the surface-exchange kinetics on the oxygen-permeation properties were studied in terms of the surface modification. The percolation threshold of the membranes for electronic conduction was also investigated to verify the minimum content of the perovskite phase.

## 2. EXPERIMENTAL METHODS

The dual-phase membranes were fabricated using tape-casting techniques. A mixture of $Ce_{0.9}Gd_{0.1}O_{2-\delta}$ (GDC10, Anan Kasei, Japan) and $La_{0.6}Sr_{0.4}Co_{0.2}Fe_{0.8}O_{3-\delta}$ (LSCF6428, Kceracell, Korea) was ball-milled in alcohol for 48 h to ensure homogeneous distribution of the two phases. The composite powders were dried using an evaporator and were ball-milled for 24 h with appropriate amounts of dispersant, plasticizer, binder, and solvent to form tape-casting slurries. The tape casting was performed using a casting device in which the slurry was coated onto a polymer carrier film. In order to control the thickness of the membrane, sheets were stacked and laminated at 70 °C under a pressure of 10 MPa. The laminated sheet was sintered at 1300 °C for 3 h to densify the dual-phase membrane. The diameter of the sintered sample was 19 mm. For surface modification of the membrane, a $La_{0.6}Sr_{0.4}CoO_{3-\delta}$ (LSC, Kceracell, Korea) coating slurry was prepared by mixing the powder with an organic solution. The coating slurry was brush-painted on both sides or only one side of the membrane, which was subsequently fired at 1000 °C. The oxygen permeation flux across the membrane was detected with a gas chromatograph (ACME 6000, YoungLin). The membranes were glass-sealed into an $Al_2O_3$ tube. For oxygen permeation measurements, synthetic air (0.21 atm) and high-purity He (99.999%) were used as the feed gas and sweeping gas, respectively, with a flow rate of 400 mL·min$^{-1}$. The gas chromatograph was calibrated using a standard gas mixture containing $N_2$ and $O_2$, with He as the balance gas. The oxygen fluxes through the membrane were corrected for leakage using the following equation

$$j_{O_2} = \left(x_{O_2} - \frac{21}{79}x_{N_2}\right)\frac{F}{A} \quad (1)$$

where $j_{O_2}$ is the oxygen flux, $x$ is the molar fraction of oxygen or nitrogen, $F$ is the volumetric flow rate of the effluent stream, and $A$ is the area of membrane. The gas leakages were less than 0.1%. The temperature dependence of oxygen fluxes of the membrane was measured between 850 and 700 °C with decreasing temperature as shown in Figure 1.

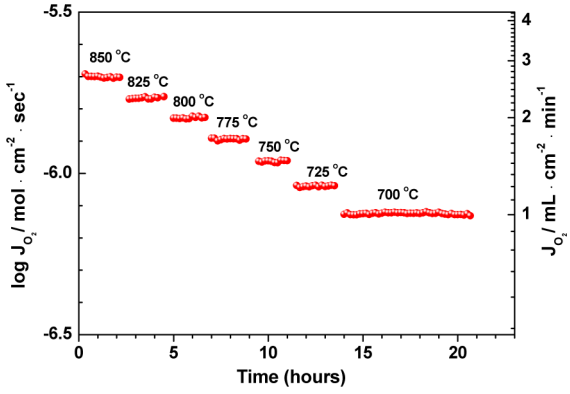


**Figure 1.** Time and temperature dependence of oxygen fluxes of the dual-phase 70 vol % GDC−30 vol % LSCF membrane (thickness~ 60 $\mu$m).

The electrical conductivities (in-plane mode) of the dual-phase membrane were measured by the two-probe DC method. Platinum paste was painted on two ends of the membrane and fired at 800 °C for 1 h. DC conductivity was measured by using a current source (K220, Keithley, USA) and a voltmeter (K196, Keithley, USA). The microstructure of the membranes was observed by a scanning electron microscope (Hitachi, Japan). The phase of the membrane was characterized by X-ray diffraction (Rigaku 2200).

## 3. RESULTS AND DISCUSSION

**3.1. Electrical Conductivity and Material Characterization.** In order to obtain the desired oxygen flux, the dual-phase membrane should consist of two continuously distributed phases: one is a predominantly ionic-conducting phase, and the other is a predominantly electronic-conducting phase. Since fluorite material as an ionic-conductor possesses thermochemical stability, it is preferable to maximize the amount of fluorite phase in the composite membranes to enhance the overall membrane stability while maintaining adequate electronic conductivity. The total electrical conductivity of the GDC−LSCF composite as a function of LSCF content is shown in Figure 2.

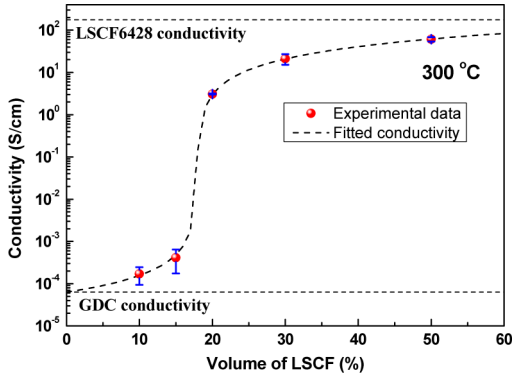


**Figure 2.** Total electrical conductivity of the GDC−LSCF composite as a function of LSCF content. Vertical error bars indicate the 95% confidence interval of the mean; when not visible, these are smaller than the symbol size.

When the individual phases had significantly different conductivities, the percolation theory could be applied to the total conductivity behavior in the dual-phase membrane. The conductivity values were fitted with a general effective-media equation (GEM), which combines most aspects of both effective media and percolation as follows:[22]

$$\frac{f(\sigma_f^{1/t} - \sigma_{tot}^{1/t})}{\sigma_f^{1/t} + (f_c/(1-f_c))\sigma_{tot}^{1/t}} + \frac{(1-f)(\sigma_p^{1/t} - \sigma_{tot}^{1/t})}{\sigma_p^{1/t} + (f_c/(1-f_c))\sigma_{tot}^{1/t}} = 0 \quad (2)$$

In eq 2, $f_c$, $f$, and $t$ are the critical volume concentration of the conductive phase (LSCF), volume fraction of the perovskite (LSCF), and exponent for the percolation, respectively; $\sigma_p$, $\sigma_f$, and $\sigma_{total}$ represent the conductivities of the perovskite (LSCF), fluorite (GDC), and composite, respectively. The terms $f_c$ and $t$ are the fitting values, and the value of $t$ is usually between 1 and 3. Exponent for the percolation ($t$) is a phenomenological parameter characterizing the percolation behavior. The $t$ value determines the effective percolation slope, which becomes steeper as the $t$ value decreases.[23] The conductivity of the composite is usually determined by the electrical conductivity


dx.doi.org/10.1021/cm501240f | Chem. Mater. 2014, 26, 4387−4394

of each phase, the relative concentration, and the morphology of the composite. The percolation behavior could be clearly observed in the dual-phase membrane since the difference in electrical conductivity beween GDC (average grain size ~1.3 $\mu$m) and LSCF (average grain size ~0.6 $\mu$m) was significant, as shown in Figure 2. In this study, the estimated percolation threshold and the percolation exponent values are 17.9% and 1.12, respectively. Therefore, 20 vol % of LSCF was determined to be sufficient for percolation of electronic conductivity in the dual-phase GDC−LSCF membrane. This result is in a good agreement with previous reports (percolation threshold of the electronic phase ~20 vol %) of the GDC− $La_{0.6}Sr_{0.4}CoO_{3-\delta}$ (GDC−LSC) composite.[24] Since the values of $t$ and $f_c$ are a function of the morphology of the composite, i.e., size, shape, space distribution, and interconnectivity, the estimated percolation threshold in this study is particularly applicable to this system. It is generally believed that a higher fraction of the fluorite phase relative to the perovskite phase is required to obtain a more stable membrane. Thus, the maximum amount of fluorite phase is preferable to enhance the overall stability of the membrane when the electronic conductivity of the dual-phase membrane is sufficient. In this study, a fluorite-rich dual-phase membrane (80 vol % GDC−20 vol % LSCF) was studied systematically as a function of membrane thickness with or without surface modification.

In Figure 3, the linear thermal expansion rates of pure LSCF and the dual-phase membrane in air and He are shown. The

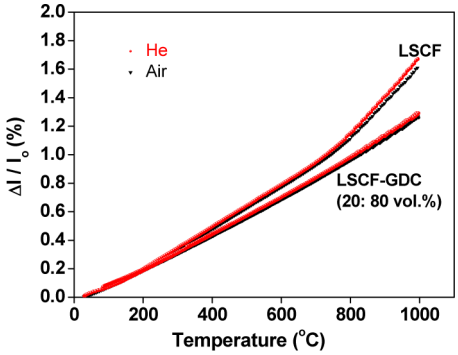


**Figure 3.** Dilatometric curves of LSCF and dual-phase membrane (80 vol % GDC−20 vol % LSCF) in air and He.

dilatometric curve of the single phase LSCF consists of two regions using a linear slope model. The thermal expansion behavior (two temperature ranges) of the LSCF can be explained by two different mechanisms. In the low temperature region (below around 700 °C, TEC: $13.8 \times 10^{-6}$ $K^{-1}$ in air and $14.4 \times 10^{-6}$ $K^{-1}$ in He), this intrinsic expansion is caused by atomic vibrations with increasing temperature. In the high temperature region (above around 700 °C, TEC: $23.3 \times 10^{-6}$ $K^{-1}$ in air and $25.1 \times 10^{-6}$ $K^{-1}$ in He), the additional contribution to the thermal expansion is induced by formation of oxygen vacancies, commonly called chemical expansion. In the case of the dual-phase membrane (80 vol % GDC−20 vol % LSCF), the chemical expansion is significantly alleviated as shown in Figure 3 due to the addition of the GDC. TEC values in the whole measured temperature (30−1000 °C) of the dual-phase membrane are $13.1 \times 10^{-6}$ $K^{-1}$ in air and $13.3 \times 10^{-6}$ $K^{-1}$ in He, respectively. This result demonstrates that the fluorite-rich dual-phase membrane has a beneficial effect on the mechanical stability.

Figure 4 shows the X-ray diffraction (XRD) pattern of the dual-phase 80 vol % GDC−20 vol % LSCF membrane after it

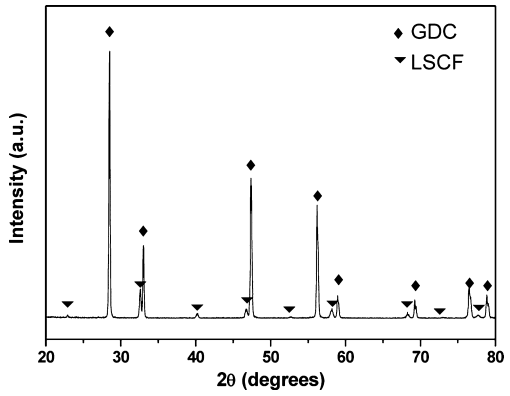


**Figure 4.** Room temperature XRD patterns of the dual-phase 80 vol % GDC−20 vol % LSCF membrane sintered at 1300 °C for 3h.

was sintered at 1300 °C for 3h. Second phases could not be detected from the XRD characterization, indicating that the sintered membrane consisted of only the GDC and LSCF phases. The lattice parameter of GDC ($a$: 5.422 Å, space group $Fm\bar{3}m$) in the membrane was slightly larger than that of pure GDC ($a$: 5.416 Å), while the unit-cell parameters of LSCF ($a$: 5.504 Å, $c$: 13.440 Å, space group $R\bar{3}c$) in the membrane were smaller than those of pure LSCF ($a$: 5.514 Å, $c$: 13.483 Å). The expansion of the lattice of GDC in the dual-phase membrane can be attributed to the diffusion of large cations (La or Sr) from the LSCF into the composite. The change in lattice parameters as a result of the interdiffusion in this study is in a good agreement with reported results in the literature.[25]

Figure 5 shows scanning electron microscope (SEM) micrographs of the dual-phase membrane that was sintered at

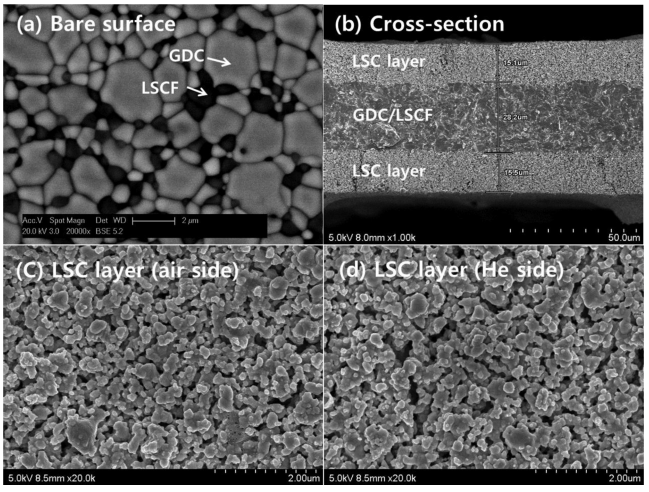


**Figure 5.** SEM images of the dual-phase 80 vol % GDC−20 vol % LSCF membrane.

1300 °C. The GDC and LSCF phases could be distinguished by backscattered SEM, and two different contrast grains were observed. The darker grain represents the LSCF phase because the amount of backscattered electrons is proportional to the atomic number. Both phases were well distributed, indicating the good chemical compatibility between the two phases. The average grain size was determined by the linear-intercept


dx.doi.org/10.1021/cm501240f | Chem. Mater. 2014, 26, 4387−4394

method from the SEM images: the grain sizes of the LSCF phase were mostly scattered in the range of 0.2 to 1 $\mu$m; the average grain sizes of GDC and LSCF were 1.4 and 0.60 $\mu$m, respectively. The cross section of the membrane film coated by LSC layers is also shown in Figure 5. Although the coating layers were brush-painted on both sides of the membrane, the variation in layer thickness was not large. Good adhesion between the membrane and the coating layers was also confirmed.

**3.2. Oxygen Flux of the Dual-Phase Membrane.** In Figure 6, the oxygen permeation fluxes of the fluorite-rich dual-

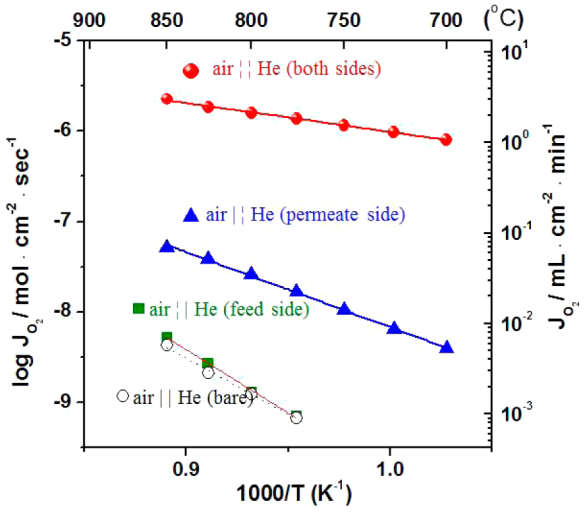


**Figure 6.** Oxygen permeation fluxes of the fluorite-rich dual-phase with and without surface modification of a $La_{0.6}Sr_{0.4}CoO_{3-\delta}$ layer.

phase membranes (80 vol % GDC−20 vol % LSCF) with and without surface modification of a $La_{0.6}Sr_{0.4}CoO_{3-\delta}$ porous layer are shown as functions of temperature under an air/He gradient. Only permeate-side (air | ¦ He) or feed-side coating (air ¦ | He) was performed in order to elucidate the mechanism of enhanced oxygen flux. Although the thickness of the membranes was only ~60 $\mu$m, the membrane with the bare surface (air | | He) exhibited a very low oxygen flux of $7.0 \times 10^{-3}$ mL·cm$^{-2}$·min$^{-1}$ at 850 °C. The activation energy for permeation of the bare membrane was calculated to be 2.76 eV, which is comparable to that for oxygen-exchange kinetics on the GDC surface (3.3 eV).[26] Considering the activation energies for surface exchange (1.39 eV) and bulk diffusion (1.55 eV)[27] of LSCF, the contribution of LSCF to the permeation of the dual-phase membrane was negligible.

In the previous literature, the bare 50 vol % GDC−50 vol % LSCF membrane (1 mm thickness) exhibited the oxygen flux of $4.7 \times 10^{-2}$ mL·cm$^{-2}$·min$^{-1}$ at 850 °C,[28] which is much higher than that of the bare membrane (80 vol % GDC−20 vol % LSCF). Even though LSCF was electronically percolated in the GDC−LSCF (80:20 vol %) composite, as shown in Figure 2, it appeared that there was no network of ionic conduction pathways throughout the LSCF phase. The electrical conductivity of the membrane with 20 vol % of LSCF was 3.1 S·cm$^{-1}$, which is only about 2% of the conductivity of single-phase LSCF (177 S·cm$^{-1}$). The conductivity of the percolated membrane was much smaller than that of single-phase LSCF after correction for the volume fraction of the LSCF. Thus, it is reasonably assumed that the fraction of percolated LSCF particles was about 2% on the basis of the conductivity measurement, and this is the reason for the very low oxygen flux in the composite membrane with a bare surface. Its low oxygen flux with high activation energy suggests that oxygen permeation of the bare fluorite-rich membrane was mostly determined by the surface-exchange kinetics of GDC and the contribution of LSCF to the permeation was negligible. The lower oxygen flux of the bare membrane (80 vol % GDC−20 vol % LSCF) than that of the bare 50 vol % GDC−50 vol % LSCF membrane in our previous study[28] is due to the sluggish surface oxygen exchange kinetics, negligible oxygen flux from the percolated LSCF phase.

The membrane with only feed-side coating (air ¦ | He) exhibited negligible change in the oxygen flux in comparison with the flux of the bare membrane. On the contrary, the oxygen fluxes through the membrane with permeate side coating (air | ¦ He) increased by about 1 order of magnitude, indicating that the surface-exchange kinetics on each surface was different. This means that the oxygen-exchange reaction for oxygen incorporation at the feed side, ($1/2\ O_2(g) + 2e^- \rightarrow O^{2-}(s)$), was not the same as the reaction for oxygen excorporation at the permeate side, ($O^{2-}(s) \rightarrow 1/2\ O_2(g) + 2e^-$). The fact that oxygen incorporation was not affected by modification of the feed side suggests that, in the composite membrane with a bare surface, the oxygen excorporation reaction at the permeate side rather than the incorporation reaction at the feed side was rate-limiting. The decreased surface-exchange kinetics with decreasing oxygen partial pressure could have been a possible reason for the more rate-limiting reaction at the permeate side. In addition, in the $P_{O_2}$ region of this study, the electronic conductivity of the GDC can be expressed by the $P_{O_2}^{1/4}$-dependent characteristic.[29] Thus, the surface modification at the permeate side enhanced the oxygen flux by the increase in lateral electronic conductivity of the GDC surface, which could facilitate the oxygen-excorporation reaction. On the contrary, the surface modification at the feed side showed negligible impact on the oxygen flux owing to the poor surface-exchange kinetics and electronic conductivity of GDC at the permeate side.

Surface coating on both sides (air ‖ He) drastically enhanced the oxygen flux by about 3 orders of magnitude. It should also be noted that the activation energy (0.64 ± 0.01 eV) of the membrane coated with LSC layers was similar to that (0.61 eV) of the ionic conductivity of GDC, which means that the oxygen transport through the membrane with surface modification was mostly governed by the GDC ionic conductivity. This result clearly demonstrates that the surface modification with a LSC porous layer drastically changed the rate-determining step in oxygen transport through the GDC-rich composite membrane from surface-exchange kinetics to bulk diffusion in the GDC phase. The surface modification of the fluorite phase played a decisive role in enhancing the contribution of the fluorite phase to the fluorite-rich dual-phase membrane. Similar study of the surface modification in the dual-phase membranes was already reported. $Ce_{0.8}Gd_{0.2}O_{2-\delta}$−$La_{0.8}Sr_{0.2}MnO_{3-\delta}$ was used to improve surface catalytic behavior.[18]

The oxygen permeation fluxes of the dual-phase (70 vol % GDC−30 vol % LSCF) and pure LSCF membranes with surface modifications by LSC (both sides) were also measured for comparison. The oxygen flux of LSCF is lower than that of GDC-LSCF composite membranes as shown in Figure 7. The ionic conductivity of $Ce_{0.9}Gd_{0.1}O_{2-\delta}$ (0.075 S/cm at 800 °C) is higher than that of $La_{0.6}Sr_{0.4}Co_{0.2}Fe_{0.8}O_{3-\delta}$ (0.008 S/cm at 800


dx.doi.org/10.1021/cm501240f | Chem. Mater. 2014, 26, 4387−4394

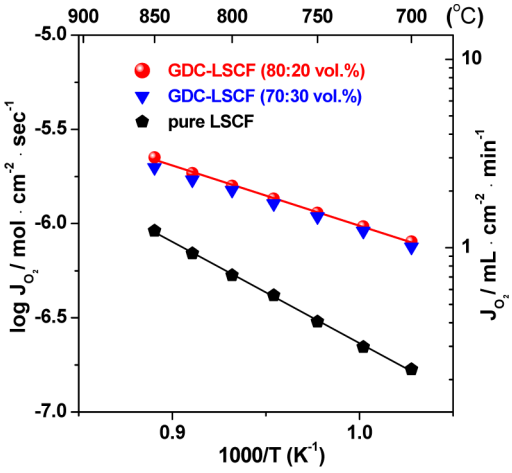


**Figure 7.** Temperature dependence of the oxygen fluxes of GDC-LSCF and pure LSCF membranes with LSC surface coatings. The thickness of the membranes was ~60 $\mu$m.

°C)[30] in air. Thus, it is expected that the oxygen flux of GDC-LSCF composite membrane is higher than that of pure LSCF when the oxygen transport is mostly determined by ionic conduction. The oxygen permeation fluxes of the membrane (80 vol % GDC−20 vol % LSCF) are slightly higher than that of the membrane (70 vol % GDC−30 vol % LSCF). This also confirms that the oxygen transport is mostly governed by ionic conduction in the surface modificated dual-phase membrane. In this study, lanthanum strontium cobaltite is used as the coating layer. A detailed comparison of the Co-free oxides with good chemical stability in a $CO_2$ containing atmosphere as the coating layer will be made in the next paper.

To explain the drastic effects of surface modification on the oxygen permeation, possible paths of oxygen incorporation into the membrane with and without surface modification were proposed during our study, as schematically shown in Figure 8.

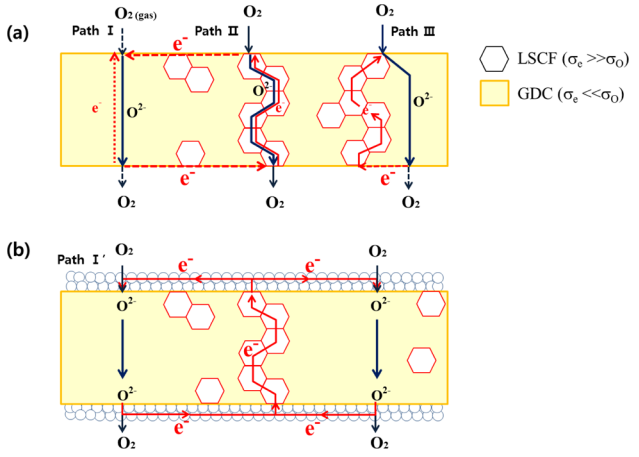


**Figure 8.** Possible paths of oxygen incorporation into the dual-phase membrane with and without surface modification.

Without the LSC coating (Figure 8(a)), the exchange would have taken place on the bare GDC surface (path I). $O_2$ was dissociated and reduced on the surface of GDC, and this was followed by the incorporation and diffusion of oxygen ions in the bulk. The rate of path I is expected to be very sluggish owing to the lack of electronic carriers in the GDC phase. In addition, the supply of electrons from the percolated LSCF phase (electronic current in lateral direction) was also limited by low electronic conductivity of GDC. The second possible path would have been located on the surface of the percolated LSCF (path II).

Oxygen reduction reaction occurred on the surface of the LSCF phase, which was relatively active to oxygen reduction. The rate of path II is expected to be relatively fast because the reported surface-exchange coefficient of LSCF (~$10^{-6}$ cm·$s^{-1}$ at 800 °C)[31] was about 3 orders of magnitude higher than that of GDC (~3 × $10^{-9}$ cm·$s^{-1}$ at 800 °C).[26] However, based on the activation energy for permeation in the bare membrane, the contribution of path II could be considered negligible because the fraction of the percolated LSCF phase was much smaller than 20 vol %. Compared to percolated LSCF, isolated LSCF particles that were not involved in electronic conduction would have been inert to oxygen incorporation. The third possible path would have taken place at the triple-phase boundary between LSCF, GDC, and oxygen gas phases (path III). Electrons transferred from the percolated LSCF to the triple-phase boundary facilitated the oxygen incorporation of GDC. For the same reason postulated for path II, however, the effective number of triple-phase boundaries was as low as the number of percolated LSCF particles on the surface. Therefore, it appears that oxygen permeation of the bare membrane was mostly determined by the reaction of path I.

Figure 8(b) shows a schematic illustration of the new path (path I′) for oxygen incorporation into the fluorite-rich dual membrane by modifying the surface on both sides. Electrons from LSCF could be rapidly distributed to the GDC surface with the aid of highly conductive LSC coating layers at the feed side, facilitating the oxygen incorporation over the entire membrane surface. On the permeate side, free electrons produced by oxygen-excorporation reaction could also be transferred to electronic paths (percolated LSCF). Mixed conducting LSC is a highly catalytic material for redox reaction of oxygen. However, it should be mentioned that, even though modification on only one side of the membrane could promote the surface reaction of path I, the lack of electronic conduction was not the primary cause of the improvement in oxygen flux. The great improvement in the oxygen permeation flux by the surface modification of both sides clearly verifies that the mixed ionic and electronic conduction was attained in the entire dual-phase membrane via the electronic conduction along the LSCF and LSC coating layers on both feed and permeate sides. Thus, the formation of an electronic short circuit on the fluorite surface played a crucial role in significant improvement of oxygen flux. It was also recently reported that the electronic short circuit is very important for oxygen permeation flux in the fluorite-based membrane.[32,33] Through the surface modification of the fluorite phase, the contribution of GDC to the dual-phase membrane in terms of oxygen transport was dramatically enhanced.

**3.3. Oxygen Surface Exchange and Ionic Conductivity of the Membrane.** In order to confirm the surface-exchange kinetics of the dual-phase membrane with surface modification, the dependence of oxygen flux on membrane thickness was investigated, as shown in Figure 9. The oxygen flux values increased with decreasing thickness of the membrane. However, as the membrane thickness was decreased, the specific flux ($J_{O_2}$·$L$) gradually decreased as well. This result clearly indicates that the surface-exchange kinetics was not


dx.doi.org/10.1021/cm501240f | Chem. Mater. 2014, 26, 4387−4394

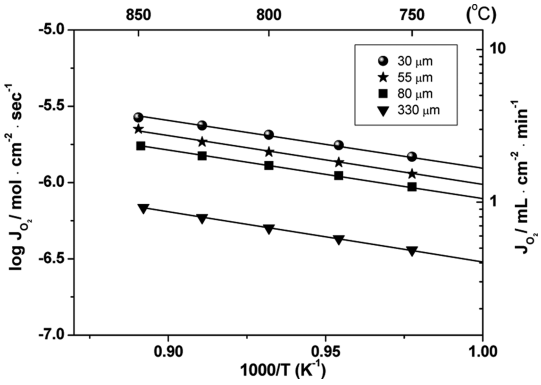


**Figure 9.** Temperature dependence of oxygen permeation flux with thickness of 30 $\mu$m, 55 $\mu$m, 80 $\mu$m, and 330 $\mu$m.

negligible in the permeation of oxygen. If the permeation was only determined by bulk diffusion, the $J_{O_2}\cdot L$ values should have remained constant as a function of thickness. Thus, in this thickness range, the effect of surface-exchange kinetics on the oxygen permeation should be considered. The ambipolar conductivity of the dual-phase membrane was controlled by the oxygen ionic conductivity of GDC when LSCF was percolated. When the permeation was limited by bulk diffusion processes, the oxygen flux through the membrane can be derived by the Wagner equation:

$$J_{O_2} \approx -\frac{RT}{16F^2L}\int_{\ln P'_{O_2}}^{\ln P''_{O_2}} \sigma_{ion}\, d\ln P_{O_2} \quad (3)$$

If the oxygen permeation flux was controlled by both bulk diffusion and surface-exchange kinetics, the oxygen flux through membrane can be described by a modified Wagner equation as follows[34]

$$J_{O_2} \approx -\frac{1}{1+(2L_C/L)}\frac{RT}{16F^2L}\int_{\ln P'_{O_2}}^{\ln P''_{O_2}} \sigma_{ion}\, d\ln P_{O_2} \quad (4)$$

where $L$ is the membrane thickness, $\sigma_{ion}$ is the ionic conductivity, $L_C$ $(= D/k)$ is the characteristic thickness, $D$ is the diffusion coefficient, $k$ is the surface-exchange coefficient, and the other symbols have their usual meanings. Here, the oxygen exchange reactions at the feed and permeate sides were not the same. Thus, the characteristic thickness can be considered as the effective characteristic thickness. Since the surface-exchange kinetics could not be negligible in this study, the modified Wagner model was applied to describe the thickness-dependent permeation behavior. Since the independent variables as functions of thickness could be fixed as constants in this measurement condition, eq 4 can be rewritten as[28]

$$J_{O_2} = \frac{1}{1+(2L_C/L)}\frac{C}{L} = \frac{C}{L+2L_C} \quad (5)$$

where $C$ is the specific oxygen flux under a fixed oxygen partial pressure gradient and temperature. Since $C$ and $L_C$ values are unknown, these values can be obtained by a nonlinear least-squares fitting. The specific oxygen flux $(C)$ and the characteristic thickness $(L_C)$ were estimated to be $2.71 \times 10^{-8}$ mol·cm·s$^{-1}$ and ~32 $\mu$m at 850 °C. The $L_C$ (or $D/k$) value of pure GDC is generally in the centimeter range ($D \sim 2 \times 10^{-8}$ cm$^2$·s$^{-1}$, k $\sim 3 \times 10^{-9}$ cm·s$^{-1}$ at 800 °C). Therefore, the effective characteristic thickness of the GDC-rich phase membrane was significantly decreased by the surface modification and electronic short circuits.

Figure 10(a) shows the oxygen permeation flux through the dual-phase membrane as a function of membrane thickness

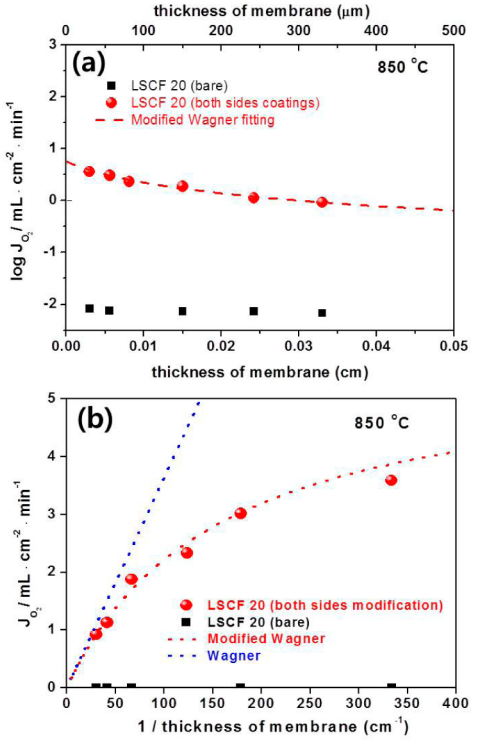


**Figure 10.** (a) Oxygen permeation flux through the dual-phase membrane as a function of membrane thickness with or without surface modification at 850 °C. (b) Oxygen fluxes derived from modified Wagner and Wagner equations as a function of the inverse membrane thickness at 850 °C.

with or without surface modification at 850 °C. The oxygen flux of the uncoated membrane was very low and was independent of the thickness. This demonstrates again that the oxygen permeation was controlled by the surface-exchange kinetics reaction. When both sides of the LSC surface were coating, the oxygen fluxes were surprisingly enhanced, with values of up to 3.6 mL·cm$^{-2}$·min$^{-1}$ at 850 °C under an oxygen gradient in air–He. To the best of our knowledge, this is the highest oxygen flux value ever reported for a dual-phase membrane.

The dotted line in Figure 10(a) is the fitting results applying the modified Wagner equation, and it exhibits good agreement with the experimental permeation data. This indicates that the permeation of the membrane with modified surfaces on both sides was controlled by both bulk diffusion and surface-exchange kinetics. Even though surface modification significantly enhanced the surface-exchange kinetics of GDC, the surface-exchange limitation on the GDC surface remained in the thickness range of 30–300 $\mu$m. For comparison, the estimated flux as a function of the inverse membrane thickness derived from the Wagner equation is also shown in Figure 10(b). Based on the Wagner equation, a linear relation should exist between the oxygen flux and inverse thickness. Using the Wagner equation, a higher permeation flux is expected because of the absence of the $L_C$ term in the denominator. Thus, further improvement of oxygen flux is expected by optimizing the surface coating in this thickness range.


dx.doi.org/10.1021/cm501240f | Chem. Mater. 2014, 26, 4387–4394

The nominal ionic conductivity can be estimated from the Wagner equation by assuming that the ionic conductivity of the membrane was independent in the range of measured values of the oxygen partial pressure. The oxygen ionic conductivity derived from the Wagner equation can be described by eq 3:

$$\sigma_{\text{ion}} = J_{O_2} \frac{16F^2}{RT} \left[ \ln\left( \frac{P_{O_2}^{high}}{P_{O_2}^{low}} \right) \right]^{-1} L \tag{6}$$

However, from the modified Wagner eq 4, the ionic conductivity can be estimated using the following equation:

$$\sigma_{\text{ion}} = J_{O_2} \frac{16F^2}{RT} \left[ \ln\left( \frac{P_{O_2}^{high}}{P_{O_2}^{low}} \right) \right]^{-1} (L + 2L_C) \tag{7}$$

Compared with the Wagner equation, the estimated nominal ionic conductivity is increased by a factor of $(L + 2L_C/L)$.

Figure 11 shows the oxygen ionic conductivities estimated from eqs 6 and 7 for the dual-phase membrane with

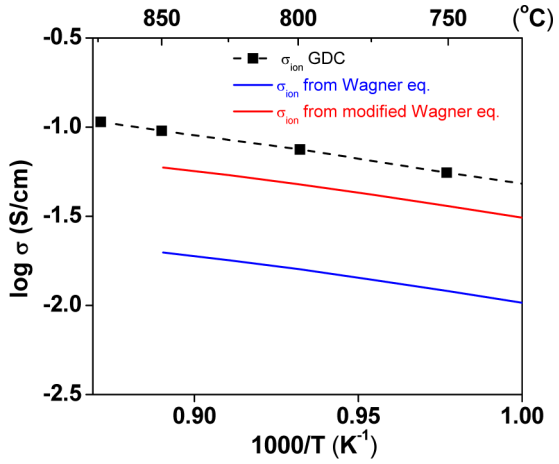


**Figure 11.** Temperature dependence of the oxygen ionic conductivities derived from modified Wagner and Wagner equations for the dual-phase membrane with surface modification, ionic conductivity for single phase GDC from DC measurement.

modification on both sides. The measured conductivities of single-phase GDC are also shown for comparison. Since the effective characteristic thickness ($L_C$) of the both sides of the coated membrane was ~32 $\mu$m at 850 °C, the value of $(L + 2L_C)/L$ at a membrane thickness of 30 $\mu$m was about 3. Since the apparent activation energy of the permeation was nearly unchanged as a function of membrane thickness, as shown in Figure 9, it is reasonably assumed that the characteristic thickness is nearly constant in the measured temperature. In this case, the conductivity estimated from eq 7 can be considered to be about 3 times larger than that estimated from eq 6. The estimated ionic conductivity of the membrane was about 60% of that of single-phase GDC. This ionic conductivity value is acceptable in view of the 80% GDC volume fraction in the dual-phase membrane. Based on this result, it is apparent that the decrease of the conductivity resulting from the interdiffusion between LSCF and GDC during sintering was not significant.

## 4. CONCLUSIONS

Fluorite-dominant dual-phase membrane with very high oxygen flux was successfully demonstrated by the tape-casting technique. The minimum amount of perovskite phase in the dual-phase membranes for electronic conduction was estimated to be about 20 vol %. The oxygen flux of the uncoated fluorite-phase-rich membrane exhibited a very low oxygen flux. However, with modification of the surface on both sides, the flux of the membrane was surprisingly improved by about 3 orders of magnitude compared with that of the membrane with nonmodified surfaces. This observation implies that the formation of an electronic short circuit at the fluorite surface as a result of surface modification on both sides played a decisive role in the dramatic improvement in oxygen permeation flux. This significant enhancement of the oxygen fluxes is of particular importance as dual-phase membranes are the most studied class of the chemical and mechanical stable membrane. This encouraging result indicates that the fluorite-dominant dual-phase membrane is a promising candidate for next-generation oxygen-permeable membranes.

## AUTHOR INFORMATION


### Corresponding Authors

*E-mail: jhjoo@kier.re.kr, jonghoonjoo@gmail.com (J.H.J.).
*E-mail: jhyu@kier.re.kr (J.H.Y.).

### Present Address

§Energy Storage Materials Research Center, Research Institute of Industrial Science and Technology (RIST), San 32, Hyoja-dong, Nam-gu, Pohang, 790-330, Republic of Korea.


### Notes

The authors declare no competing financial interest.

## ACKNOWLEDGMENTS

This work was conducted under the framework of Research and Development Program of the Korea Institute of Energy Research (KIER) (B4-2442-01).

## REFERENCES


(1) Buhre, B. J. P.; Elliott, L. K.; Sheng, C. D.; Gupta, R. P.; Wall, T. F. *Prog. Energy Combust.* **2005**, *31*, 283.
(2) Lawal, A.; Wang, M.; Stephenson, P.; Yeung, H. *Fuel* **2009**, *88*, 2455.
(3) Figueroa, J. D.; Fout, T.; Plasynski, S.; Mcllvried, H.; Srivastava, R. D. *Int. J. Greenhouse Gas Control* **2008**, *2*, 9.
(4) Merkel, T. C.; Lin, H.; Wei, X.; Baker, R. *J. Membr. Sci.* **2010**, *359*, 126.
(5) Kunze, C.; Spliethoff, H. *Appl. Energy* **2012**, *94*, 109.
(6) Sunarso, J.; Liu, S.; Lin, Y. S.; Diniz da Costa, J. C. *Energy Environ. Sci.* **2011**, *4*, 2516.
(7) Liu, Y.; Zhu, X.; Li, M.; Liu, H.; Cong, Y.; Yang, W. *Angew. Chem., Int. Ed.* **2013**, *52*, 3232.
(8) Zhang, K.; Shao, Z.; Li, C.; Liu, S. *Energy Environ. Sci.* **2012**, *5*, 5257.
(9) Shao, Z.; Yang, W.; Cong, Y.; Dong, H.; Tong, J.; Xiong, G. *J. Membr. Sci.* **2000**, *172*, 177.
(10) Shao, Z.; Haile, S. M. *Nature* **2004**, *431*, 170.
(11) Schulze-Küppers, F.; Baumann, S.; Meulenberg, W. A.; Stöver, D.; Buchkremer, H.-P. *J. Membr. Sci.* **2013**, *433*, 121.
(12) Arnold, M.; Wang, H.; Feldhoff, A. *J. Membr. Sci.* **2007**, *293*, 44.
(13) Waindich, A.; Möbius, A.; Müller, M. *J. Membr. Sci.* **2009**, *337*, 182.
(14) Luo, H.; Efimov, K.; Jiang, H.; Feldhoff, A.; Wang, H.; Caro, J. *Angew. Chem., Int. Ed.* **2011**, *50*, 759.

(15) Zhu, X.; Liu, H.; Cong, Y.; Yang, W. *Chem. Commun.* **2012**, *48*, 251.
(16) Luo, H.; Jiang, H.; Klande, T.; Cao, Z.; Liang, F.; Wang, H.; Caro, J. *Chem. Mater.* **2012**, *24*, 2148.
(17) Wang, Y.; Hu, B.; Zhu, Z.; Bouwmeester, H. J. M.; Xia, C. *J. Mater. Chem. A* **2014**, *2*, 136.
(18) Balaguer, M.; García-Fayos, J.; Solís, C.; Serra, J. M. *Chem. Mater.* **2013**, *25*, 4986.
(19) Kharton, V. V.; Kovalevsky, A. V.; Viskup, A. P.; Figueiredo, F. M.; Yaremchenko, A. A.; Naumovich, E. N.; Marques, F. M. B. *J. Electrochem. Soc.* **2000**, *147*, 2814.
(20) Wu, K.; Xie, S.; Jiang, G. S.; Liu, W.; Chen, C. S. *J. Membr. Sci.* **2001**, *188*, 189.
(21) Yi, J.; Zuo, Y.; Liu, W.; Winnubst, L.; Chen, C. *J. Membr. Sci.* **2006**, *280*, 849.
(22) McLachlan, D. S.; Blaszkiewicz, M.; Newnham, R. E. *J. Am. Ceram. Soc.* **1990**, *73*, 2187.
(23) Han, D. G.; Choi, G. M. *Solid State Ionics* **1998**, *106*, 71.
(24) Seeharaj, P.; Berenov, A.; Raj, E.; Rudkin, R.; Atkinson, A. *Solid State Ionics* **2011**, *192*, 638.
(25) Shaula, A. L.; Kharton, V. V.; Marques, F. M. B.; Kovalevsky, A. V.; Viskup, A. P.; Naumovich, E. N. *J. Solid State Electrochem.* **2006**, *10*, 28.
(26) Lane, J. A.; Kilner, J. A. *Solid State Ionics* **2000**, *136*−*137*, 927.
(27) Esquirol, A.; Kilner, J. A.; Brandon, N. *Solid State Ionics* **2004**, *175*, 63.
(28) Joo, J. H.; Park, G. S.; Yoo, C.-Y.; Yu, J. H. *Solid State Ionics* **2013**, *253*, 64.
(29) Lübke, S.; Wiemhöfer, H.-D. *Solid State Ionics* **1999**, *117*, 229.
(30) Ullmann, H.; Trofimenko, N.; Tietz, F.; Stöver, D.; Ahmad-Khanlou, A. *Solid State Ionics* **2000**, *138*, 79.
(31) Esquirol, A.; Kilner, J. A.; Brandon, N. *Solid State Ionics* **2004**, *175*, 63.
(32) Zhang, K.; Liu, L.; Shao, Z.; Xu, R.; Diniz da Costa, J. C.; Wang, S.; Liu, S. *J. Mater. Chem. A* **2013**, *1*, 9150.
(33) Joo, J. H.; Yun, K. S.; Yoo, C.-Y.; Yu, J. H. *J. Mater. Chem. A* **2014**, *2*, 8174.
(34) Bouwmeester, H. J. M.; Kruidhgof, H.; Burggraaf, A. J. *Solid State Ionics* **1994**, *72*, 185.